COMSOL CONFERENCE EUROPE 2012

Department of Energy Engineering

University of Florence

A Simplified Numerical Model for Simulating Sliding Door and Surgical Staff Movement in an Operating Theatre

Carla Balocco

Department of Energy Engineering – University of Firenze – Italy

Excerpt from the Proceedings of the 2012 COMSOL Conference in Milan

This work deals with a numerical investigation on sliding door and people moving effects on the indoor climate of a standard ISO5 class OT with an ultraclean air filter system and a total ceiling unidirectional diffuser.

A simple method to analyze the effects on the OT climate by different sliding door conditions combined with crossing persons and persons with a stretcher crossing is provided.

The proposed procedure consists in defining some user-defined logical functions in COMSOL Multiphysics models.

In recent years several studies have focused on computational models using fluid dynamics approaches to investigate airflow patterns and the related spreading of infection in isolation and hospitalization rooms and in particular in OTs for different ventilation systems (for example operating under open or closed-door conditions)

THE BACKGROUND

Simulation of object or person movements can be handled **directly or indirectly**.

Direct simulation includes the real movement of the real "object" inside the solution domain and requires a moving mesh approach in order to be realized.

Direct simulation of the moving object requires very expensive computational cost. They are related on the one hand to the degrees of freedom increasing for a chosen number on mesh nodes, and on the other to the re-meshing procedure, often needed during computations.

The basic principle of the **indirect simulation** of a moving object in surrounding air consists otherwise in keeping into account the effects of the object's movement on the air flow.

THE ISO5 CLASS O.T. CASE STUDY

Starting from these important recent research and literature evidence **an ISO5 class OT** with **ultra clean air filters systemclimate changing due** to **different sliding doors conditions and surgical staff crossing was investigated.**

The operating room is 6.3 m wide, 6.3 m long and total volume of 119.07 m^3.

All the internal partition walls have a thermal transmittance of 2.33 W/(m^2K).

The sliding door clear opening of the O.T. is 900 mm x 2100 mm with a thickness of 40 mm, representative of a door made by an aluminium frame and a galvanized steel sheet panel with a finished powder coating.

The HVAC plant systems meets the standard requirements provided in table

Effective surface (>90% floor area)	36 m^2
ACH (Air Change per Hour)	200 1/h
Min air change flow rate	1500 m^3/h
ventilation air flow rate	23814 m^3/h
Recirculation air flow rate	22314 m^3/h
Mean inlet velocity	0.184 m/s
Minimum over-pressure differential	5 Pa

The internal air temperature of the OT was set at 20 °C and that of all the surrounding zones (T_{ext}) is assumed at 26 °C as suggested. Dimension and design parameters of the air extraction grids are reported in Table

Total number of diffusers	8 [-]
Width	0.35 [m]
Length	0.6 [m]
Effective surface	0.21 [m^2]
Total extraction area	1.68 [m^2]
Mean outlet velocity	3.94 [m/s]

The position of furniture, basic safety lighting systems, surgical lighting and surgical staff was disregarded.

The total thermal power released by 8 persons was taken a 920 W, for general lighting 400 W and for surgical equipment 1 kW;

metabolic rate was assumed 2Met (walking), that corresponds to a specific heat source of 1300 W/m^3.

Physical properties assumed for fluid, walls and solid are provided in Table

	S.I Unit	"Fluid"	"Solid"	Wall
ρ	[kg/m³]	1.2	900	600
ρ	[Pa s]	5E-5	1E+5	-
k	[W/(m K)]	0.62	0.6	0.16
C_p	[J/(kg K)]	1004	2000	840

The geometry of the studied system is outlined in Figure

The OT is accessible from a 3 m breadth adjacent corridor by a two-panels sliding door, represented in blue.

Its geometrical symmetry with respect to the mid *ZX*-plane, allows to consider one half of the studied system for computations.

This assumption was validated by some preliminary tests that were carried-out by considering the full geometry of the system.

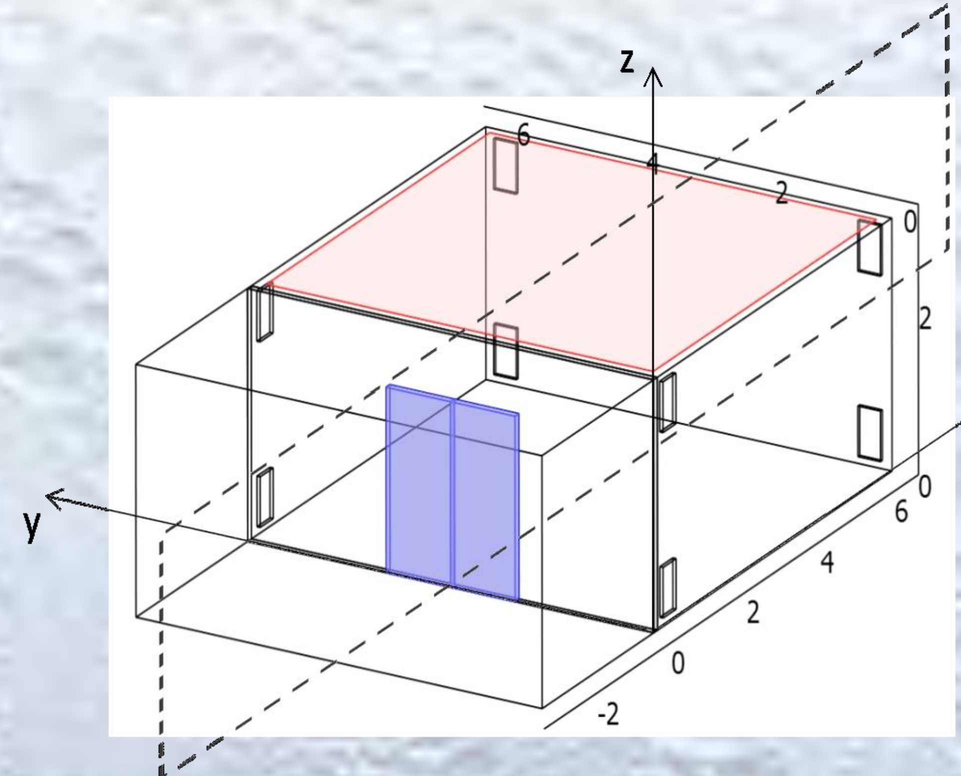

Symmetry Tests – ZX Plane – Closed Door

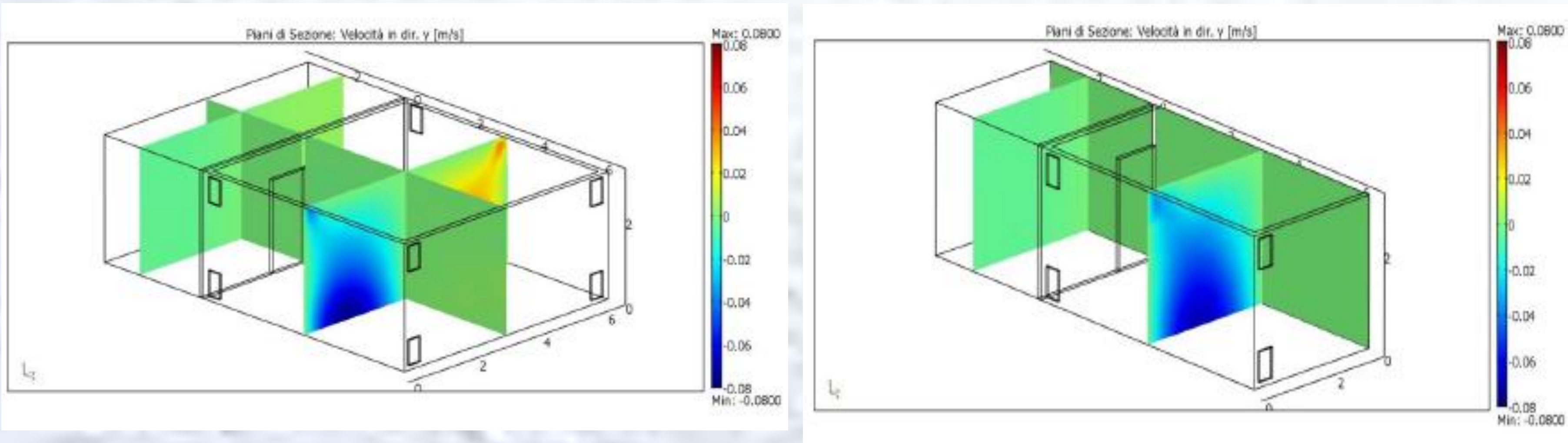

Velocity Field (Fig. a,b)

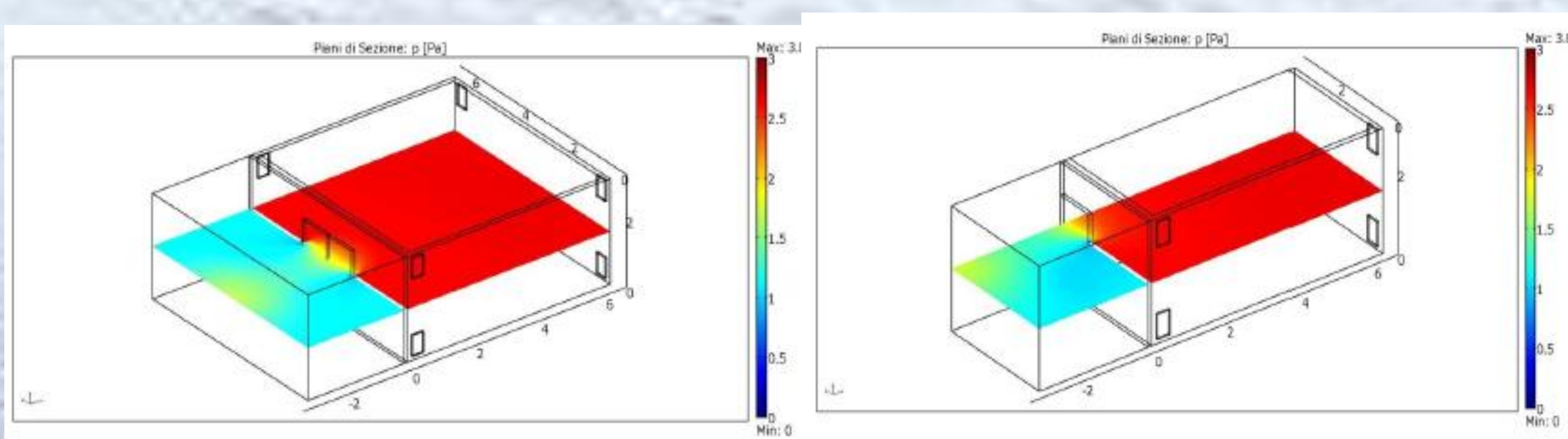

Pressure Field (Fig. c,d)

SYMMETRY TESTS – ZX PLANE – OPEN DOOR

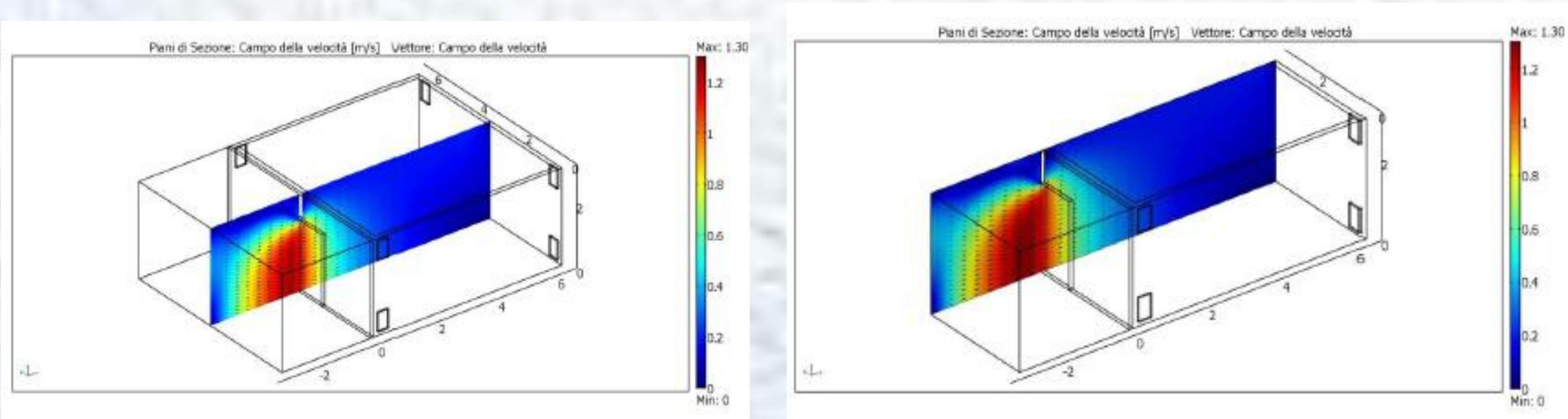

Velocity Field (Fig. e,f)

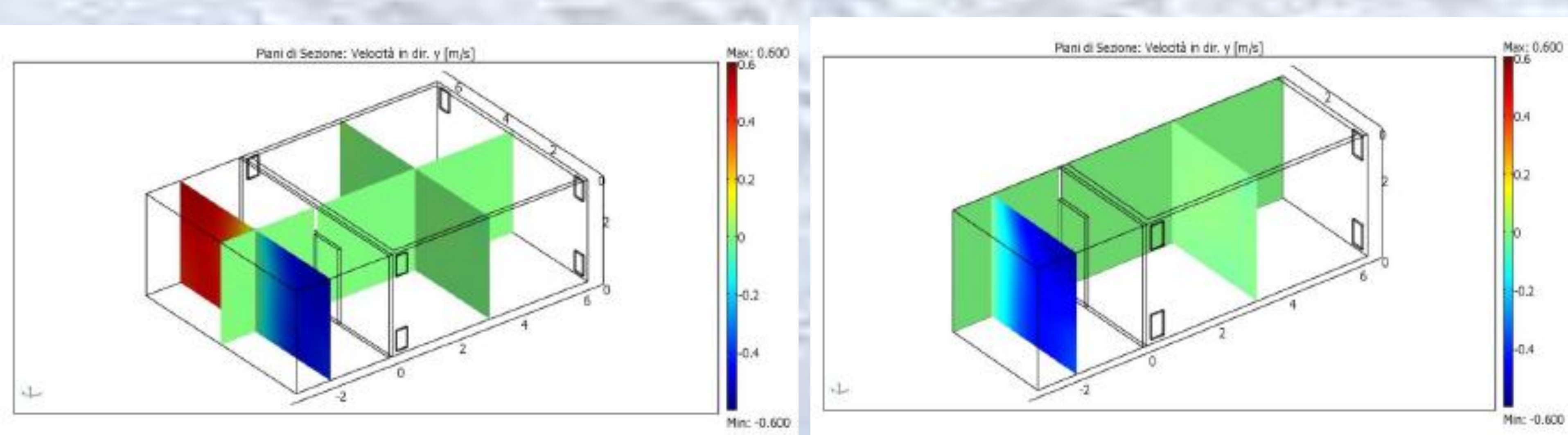

Pressure Field (Fig. g,h)

NUMERICAL MODEL AND TRANSIENT SIMULATIONS

The adopted procedure is based on the definition of specific source terms in the governing equations, with assigned values in the portions of the computational domains where the solid objects are located at a chosen time.

Moving of interfaces describing the position of the solid object is driven by some logical functions that allow simulating of the dynamics associated with the sliding door opening/closing and persons walking across the OT.

Time-dependent functions allow modification of the geometrical coordinates identifying the position of the “solid” objects during time.

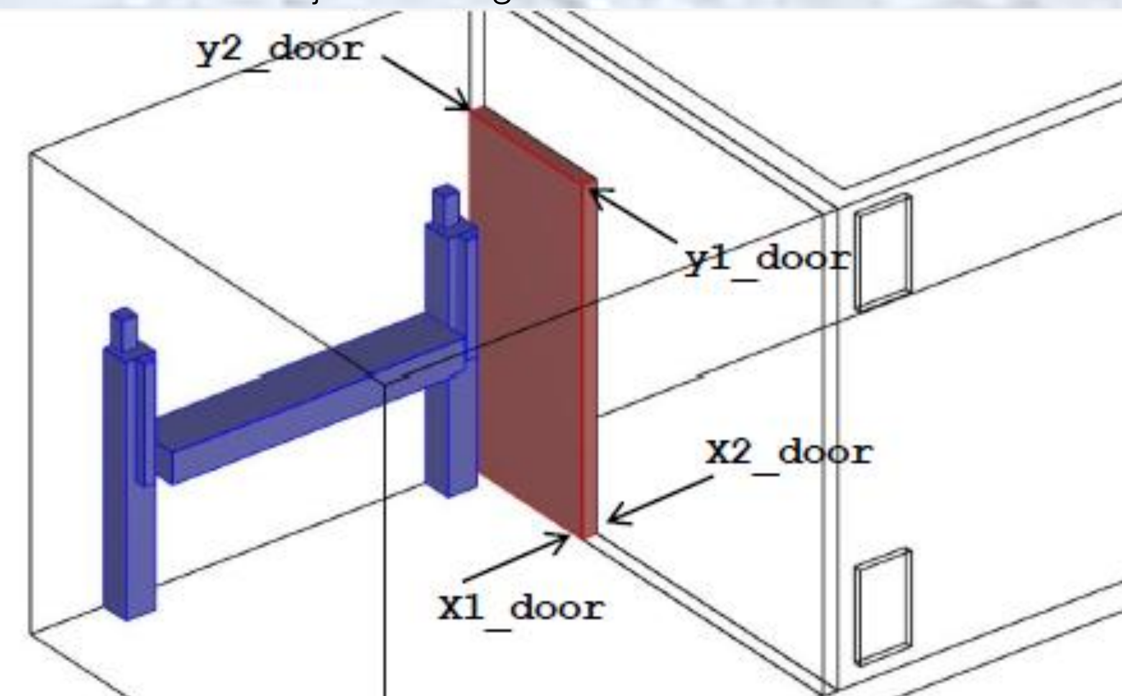

LOGICAL FUNCTIONS

x1_door	x10_door
x2_door	x20_door
y1_door	y10_door
y2_door	y20_door
z1_door	z10_door
z2_door	z20_door
x_door	if ((x>x1_door) && (x<x2_door), 1, 0)
y_door	if ((y>y1_door) && (y<y2_door), 1, 0)
z_door	if ((z>z1_door) && (z<z2_door), 1, 0)
door	x_door*y_door*z_door

Numerical Model and Transient Simulations

To investigate the turbulent air flow inside the OT, the Reynolds Averaged Navier-Stokes and energy equations were numerically solved under the assumption of Newtonian fluid and uncompressible flow.

Momentum equations are coupled with a standard k-**ε** closure scheme applied in order to model turbulence by an eddy viscosity approach. Continuous equations used are as following:

$$\rho\frac{\partial \mathbf{U}}{\partial t}+\rho(\mathbf{U}\cdot\nabla)\mathbf{U}=\nabla\cdot\left[-p\mathbf{I}+(\mu+\mu_T)\left(\nabla\mathbf{U}+(\nabla\mathbf{U})^{\mathrm{T}}\right)\right]+F_{dom} \tag{1}$$

$$\nabla\cdot\mathbf{U}=0 \tag{2}$$

$$\rho\frac{\partial k}{\partial t}+\rho\mathbf{U}\cdot\nabla k=\nabla\cdot\left[\left(\mu+\frac{\mu_T}{\sigma_k}\right)\nabla k\right]+\frac{1}{2}\mu_T\left[\nabla\mathbf{U}+(\nabla\mathbf{U})^{\mathrm{T}}\right]^2-\rho\varepsilon \tag{3}$$

$$\rho\frac{\partial \varepsilon}{\partial t}+\rho\mathbf{U}\cdot\nabla \varepsilon=\nabla\cdot\left[\left(\mu+\frac{\mu_T}{\sigma_\varepsilon}\right)\nabla \varepsilon\right]+\frac{1}{2}C_{\varepsilon 1}\frac{\varepsilon}{k}\mu_T\left[\nabla\mathbf{U}+(\nabla\mathbf{U})^{\mathrm{T}}\right]^2-\rho C_{\varepsilon 2}\frac{\varepsilon^2}{k} \tag{4}$$

$$\rho C_p\frac{\partial T}{\partial t}+\rho C_p\mathbf{U}\cdot\nabla T=\nabla\cdot(\lambda\nabla T)+Q_{dom} \tag{5}$$

$\mu_T = \rho C_\mu k^2/\varepsilon$ represents the turbulent viscosity. Values adopted for constants of the adopted mathematical model are determined from experimental data and reported in Table

C_μ	$C_{\varepsilon 1}$	$C_{\varepsilon 2}$	σ_k	σ_ε
0.09	1.44	1.92	1.0	1.3

Eq.	Boundary condition	
(1-2)	Inlet	Symmetry
	$\mathbf{U} = -U_{in}\mathbf{n}$	$\mathbf{n}\cdot\mathbf{U} = 0$ $\mathbf{t}\cdot\left[-p\mathbf{I} + (\mu+\mu_T)\left(\nabla\mathbf{U} + (\nabla\mathbf{U})^{\mathrm{T}}\right)\right]\mathbf{n} = 0$
	Output	Open
	$\left[(\mu+\mu_T)\left(\nabla\mathbf{U} + (\nabla\mathbf{U})^{\mathrm{T}}\right)\right]\mathbf{n} = 0$ $p = p_{out}$	$\left[-p\mathbf{I} + (\mu+\mu_T)\left(\nabla\mathbf{U} + (\nabla\mathbf{U})^{\mathrm{T}}\right)\right]\mathbf{n} = 0$
	Wall	
	$\mathbf{n}\cdot\mathbf{U} = 0$ $\left[(\mu+\mu_T)\left(\nabla\mathbf{U} + (\nabla\mathbf{U})^{\mathrm{T}}\right)\right]\mathbf{n} = \left[\rho C_\mu^{0.25} k^{0.5} / \left(\ln\left(\delta_w^+\right)/\kappa + C^+\right)\right]\mathbf{U}$	
(3)	Inlet	Symmetry
	$k = 3/2\left(I_T U_{in}\right)^2$	$\mathbf{n}\cdot\left[(\mu + \mu_k/\sigma_k)\nabla k - \rho\mathbf{U}k\right] = 0$
	Output / Open	Wall
	$\mathbf{n}\cdot\nabla k = 0$	$\mathbf{n}\cdot\nabla k = 0$
(4)	Inlet	Symmetry
	$\varepsilon = C_\mu^{0.75}\left(3/2\left(I_T U_{in}\right)^2\right)^{1.5} / L_T$	$\mathbf{n}\cdot\left[(\mu + \mu_T/\sigma_\varepsilon)\nabla\varepsilon - \rho\mathbf{U}\varepsilon\right] = 0$
	Output / Open	Wall
	$\mathbf{n}\cdot\nabla\varepsilon = 0$	$\varepsilon = \rho C_\mu k^2 / \left(\kappa\delta_w^+\mu\right)$
(5)	Inlet	Symmetry / Insulation
	$T = T_{in}$	$\mathbf{n}\cdot(\lambda\nabla T) = 0$
	Output	Dispersion
	$\mathbf{n}\cdot(\lambda\nabla T) = 0$	$\mathbf{n}\cdot(\lambda\nabla T) = h_{conv}\left(T_{ext} - T\right)$

Logarithmic wall functions were applied in the near wall flow, that has been considered parallel to the wall and being in a wall offset equal to one half of the boundary mesh element dimension.

The equivalent wall offset in viscous unit is defined as

$$\delta_w^+ = \delta_w \rho U_\tau / \mu$$

U_τ the frictional velocity.

Values for the constant C+ is assumed 5.5 when: $\mathrm{Re} \approx 1.5E+4$

The Karman's constant value was set equal to 0.42.

A turbulent length scale of 0.01 m and a 5% of turbulent intensity were applied at the air inlet section

The procedure mainly consists in defining some logical functions assuming binary values that identify the portions of domain where solid objects are located (binary value 1) or not (binary value 0) at the initial time.

The binary value assumed by the logical functions depends on assigned geometrical coordinates for each object.

In those regions fluid-dynamical properties and source terms assume specific values determining rest conditions for fluid.

Continuous equations were spatially discretized by FEM based on the Galerkin method on non-uniform and non-structured computational grids made of tetrahedral Lagrange second order elements.

Influence of spatial discretization was studied to assure mesh-independent results: then a mesh of 250 000 tetrahedral elements was used for transient simulations

The Galerkin Least-Squared (GLS) method was employed to prevent rising and propagation of numerical instabilities.
PARDISO direct solver was used. Computations were carried-out on a workstation disposing of two 64-bit quad-core processors speeding up to 3GHz of frequency and handling 32GB of RAM

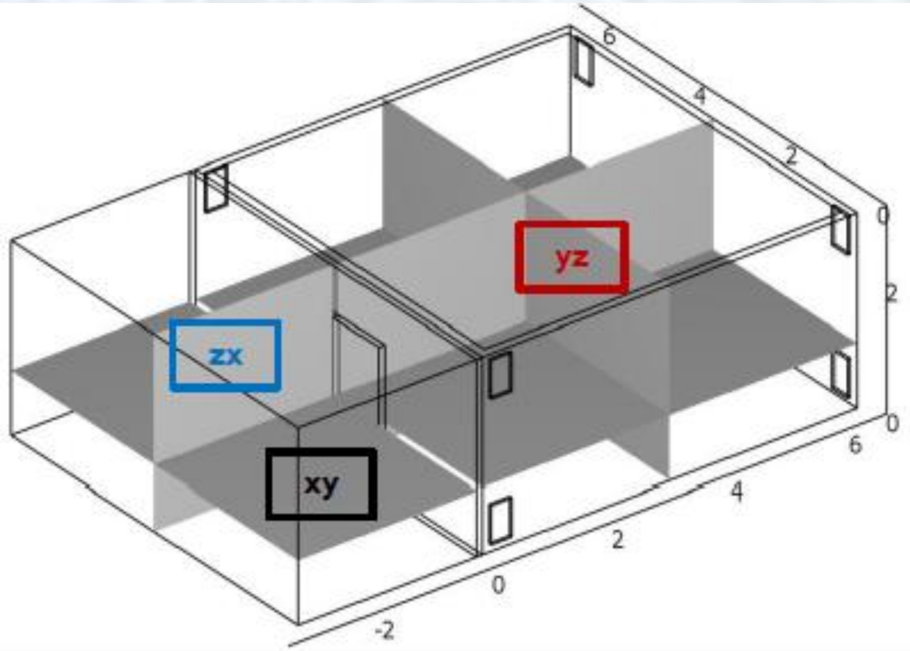

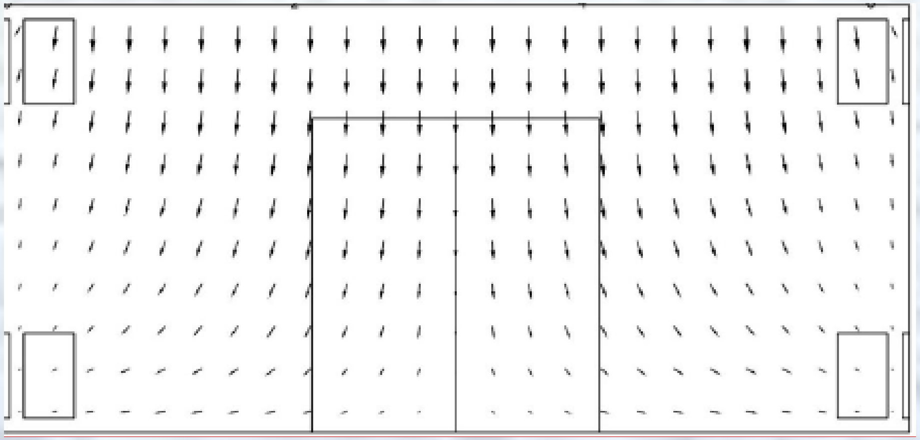

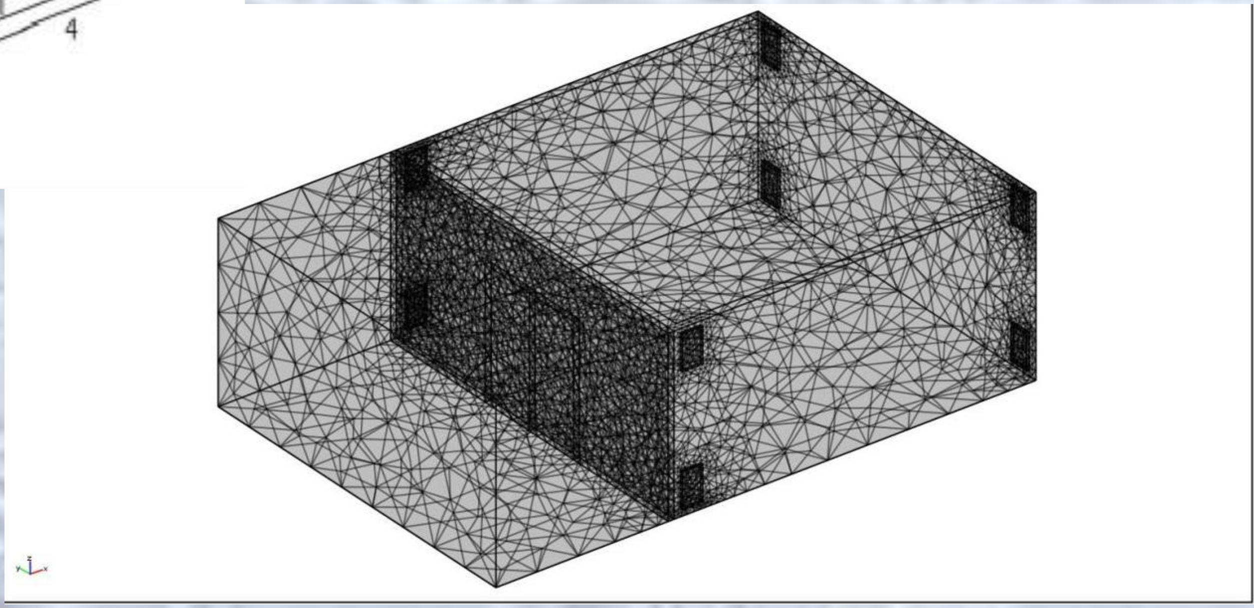

SIMULATIONS WERE PERFORMED FOR 3 CASES:

1 OPENING AND CLOSING OF THE SLIDING DOOR (CASE A)

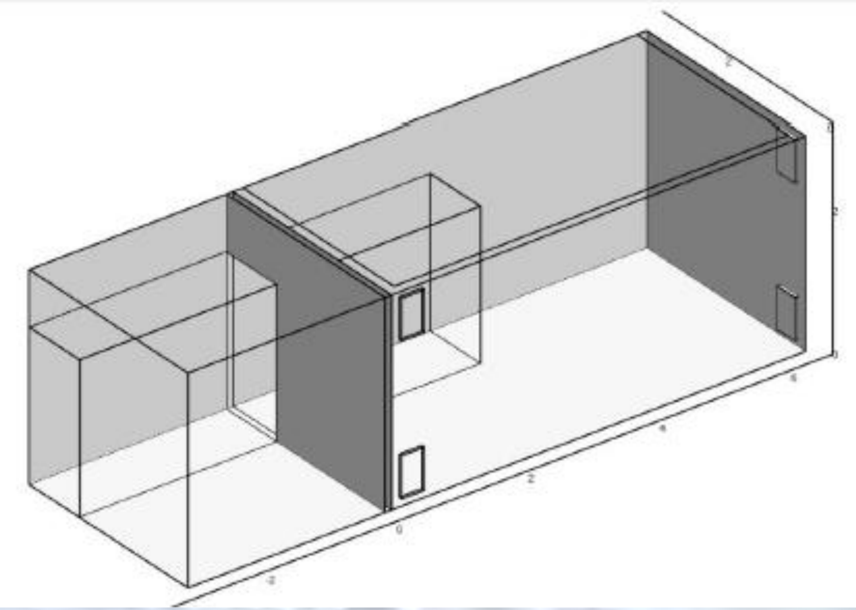

CASE A - MODEL GEOMETRY

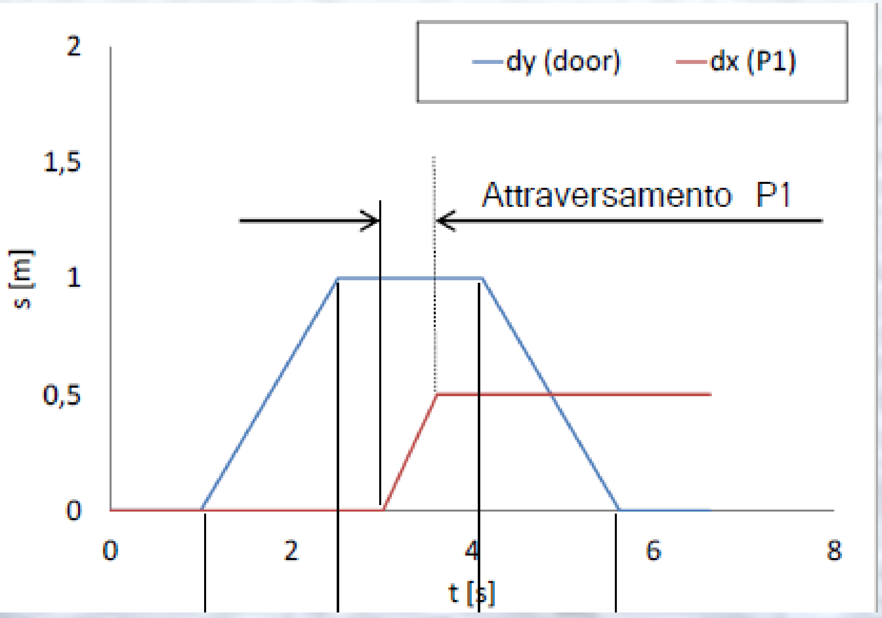

OPENING CLOSING

CASE A – SLIDING DOOR MOVEMENTS

2 OPENING OF THE SLIDING DOOR, ONE PERSON CROSSING, CLOSING OF THE SLIDING DOOR (CASE B)

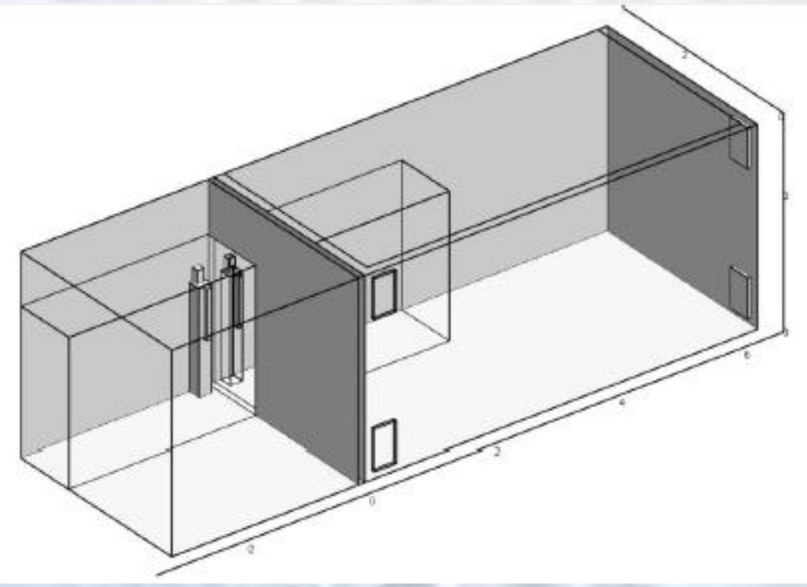

CASE B - MODEL GEOMETRY

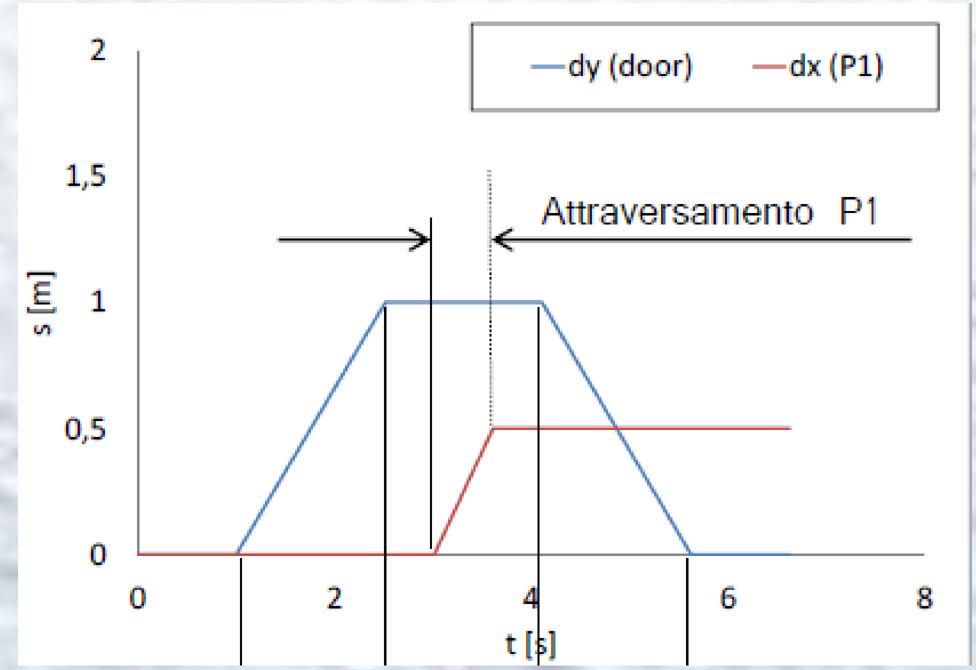

OPENING

CLOSING

CASE C – PEOPLE MOVEMENTS/CROSSING

3. Opening of the sliding door, two persons with a stretcher crossing, closing ofthe sliding door (Case C).

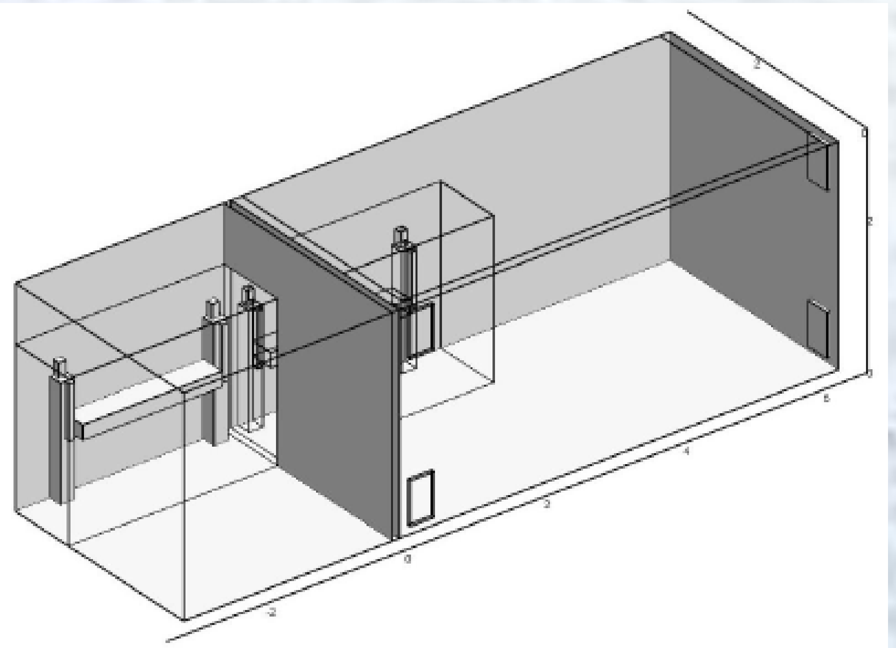

Case C - Model geometry

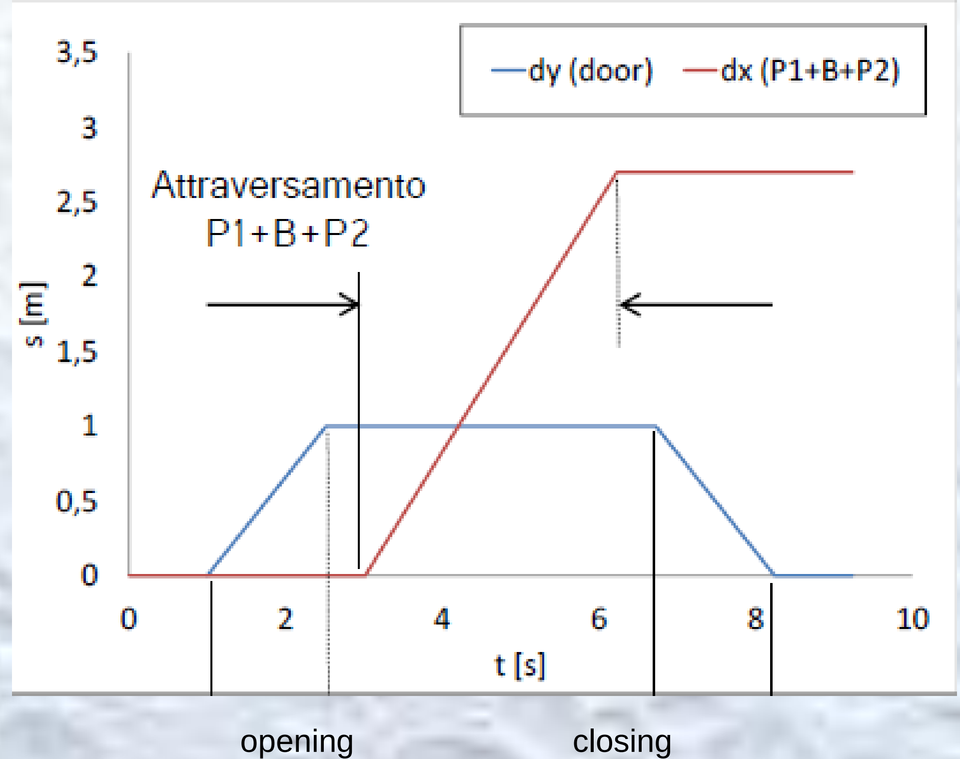

Case C – People and litter movements/crossing

Validation of the adopted numerical scheme was preliminary performed in order to check the reliability of the provided numerical results

Steady solutions of the system, used as initialisation state for transient simulations, were performed taking into account the closed sliding door and the person/s and stretcher standing in front of the door on the corridor side.

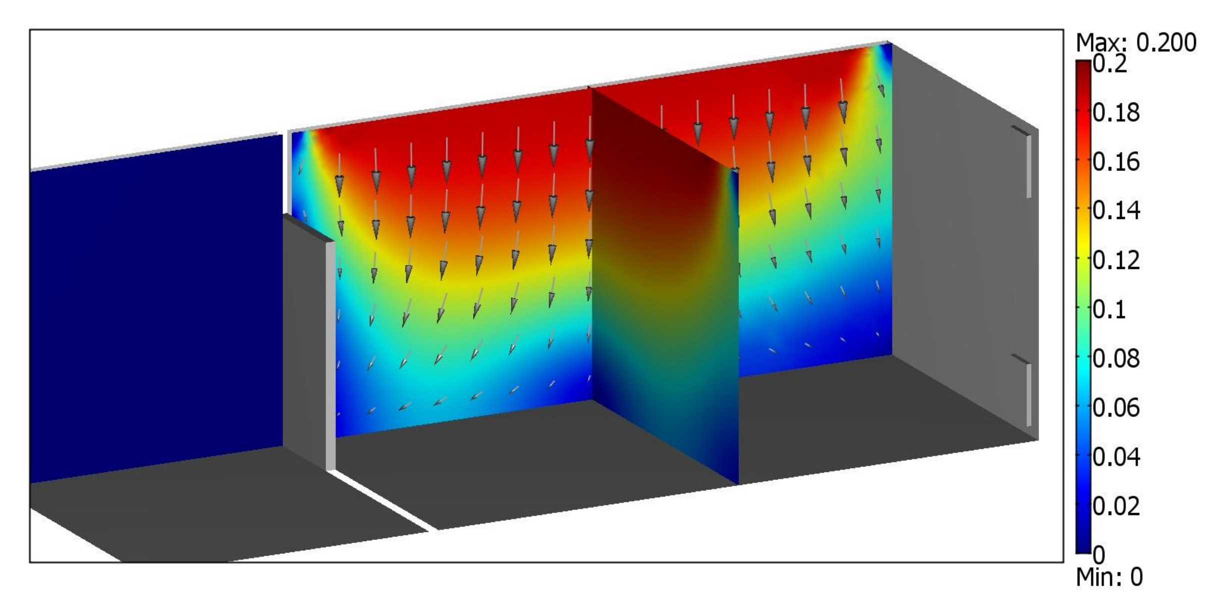

Fig. 2 Steady velocity [m/s] and velocity vectors in vertical sections

The efficiency of the ventilation system is particularly evident:
in the central zone of the OT, usually occupied by the surgical bed and staff, the plant guarantees appropriate conditions in terms of flow pattern and air velocity magnitude.

The flow is almost unidirectional, from the ceiling to the ground, highlighting the total absence of any recirculation zone and turbulence air distribution all over the room volume.

The velocity field simulated magnitude respects the indoor limits suggested as admissible by the most important standards (0.15-0.2 m/s).

At closed door conditions, the average air pressure inside the OT remains stable and uniform.
The over-pressure value respects the standard limits of 15-20 Pa, Fig. 3.

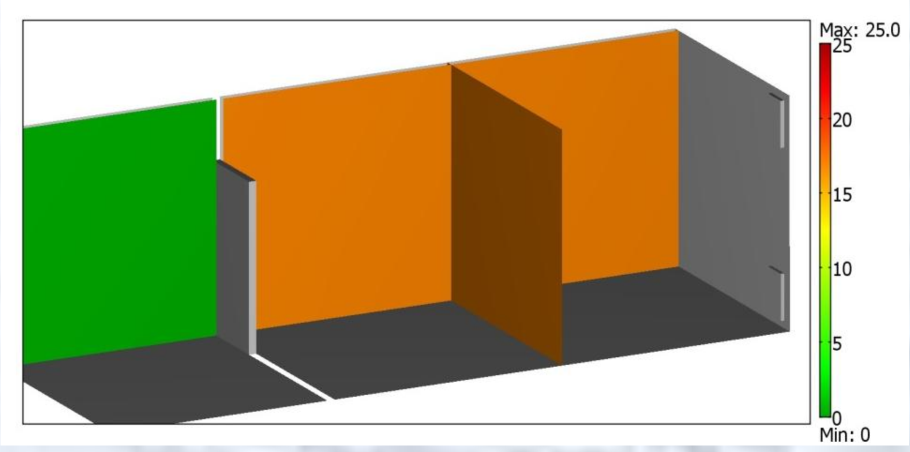

Fig. 3 Steady pressure [Pa] in vertical sections

Fig. 4 shows the temperature distribution field is very uniform in the whole air volume and its average value is 20 °C as suggested by standards.

In the zone of the partition wall facing the corridor, the isothermal line distribution highlights the local heat flux

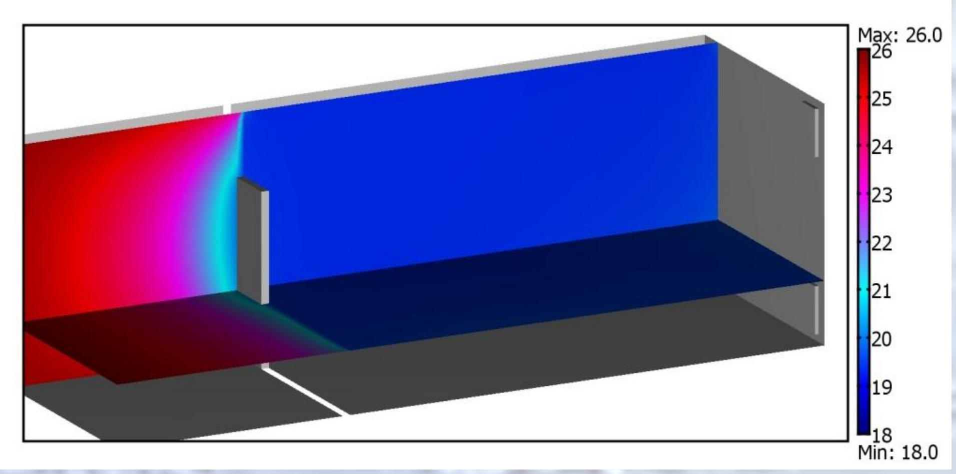

Fig. 4 Temperature [°C] in vertical and horizontal sections.

Due to the pressure level a flow rate of air from the room to the corridor is highlighted when the door opens.

The maximum magnitude of the flow velocity is reached for a partial opening position of the door.

Simulation results show air distribution reaching values of velocity magnitude up to 1.5 m/s.

Fig. 5 shows the velocity field and the velocity vectors in a horizontal slice of the OT (1.5 meters from the floor) during the door opening in the Case A.

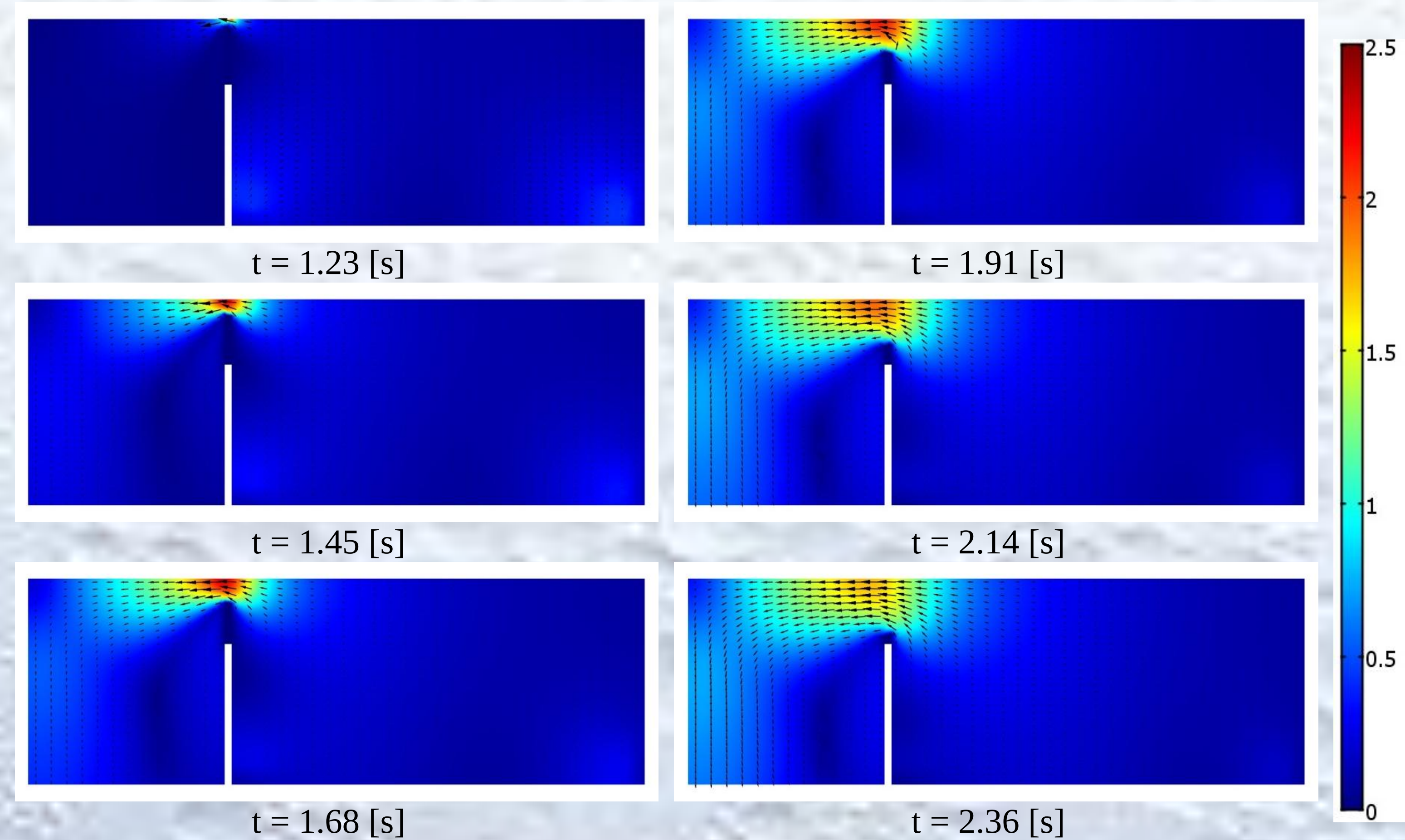

Fig. 5 Velocity field [m/s], velocity vectors in horizontal plane (z = 1.5) at several time instants during the door opening (Case A).

For the three cases studied A,B,C the effect of the door opening on the pressure levels inside the OT were estimated.

Pressure variation due to the door opening are important and cause a pressure reduction from 17 Pa to 4 Pa, that represents the limit imposed by the most restrictive standards.

In all the cases studied (A,B,C) the pressure trend, evaluated in the middle of the room at 1 m from the floor, is very similar (Fig 6, not-filled symbols).

The pressure variations were also evaluated in the plane section of the door, for the three cases during the opening condition, at 1 m from the floor (Fig. 6, filled symbols).

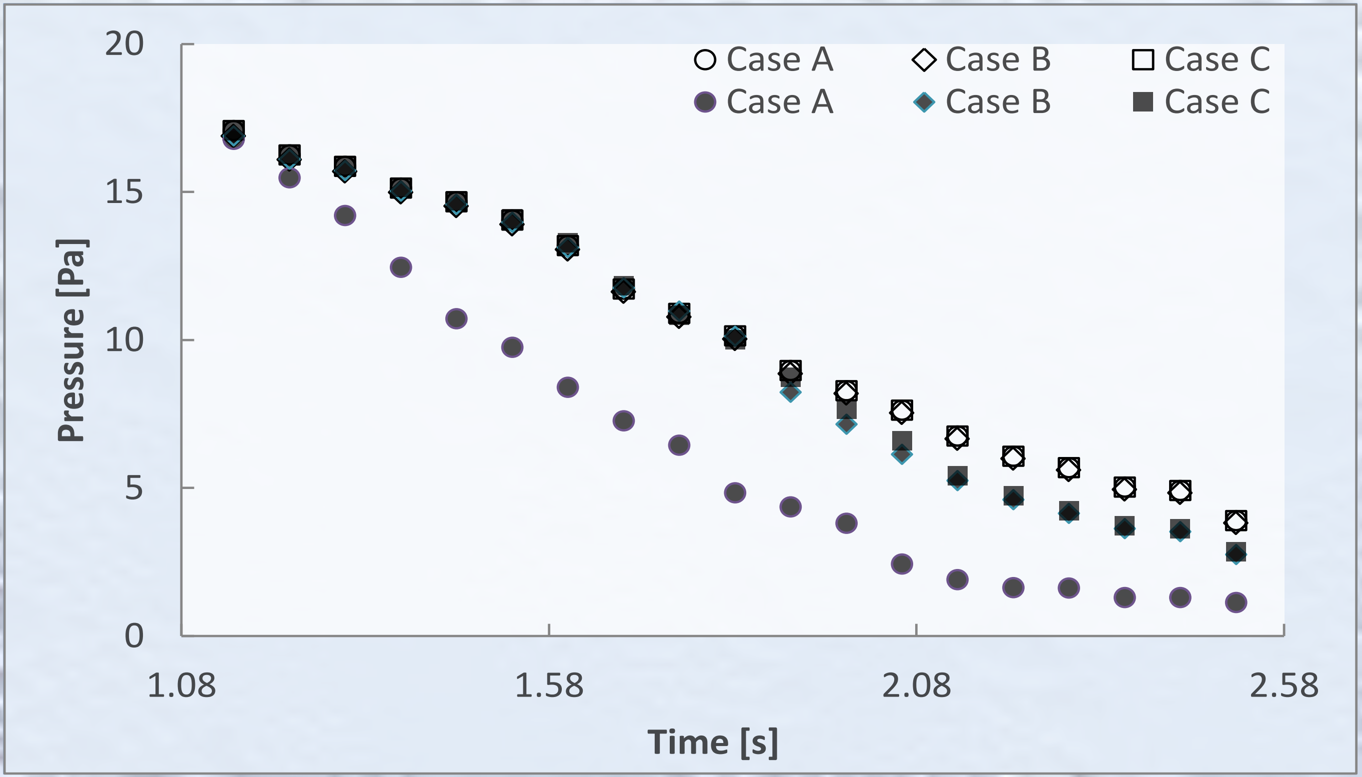

Figure 6

Time evolution of pressure during the door opening for the three case studies

The air flow rate crossing the door was also computed during the transient analyses in the three case studies.

Time evolutions of the air flow rate (Fig.7) is different for the cases studied.

For case A (continuous line), when the door is open, the outgoing air flow rate increases and spreads to the border of the open door. Then it decreases together when the door is closed. For case B, when the door is open, the air flow rate goes outside the room.

The curve slope (dashed line) is lower compared with case A, because person presence is a real obstacle to the air flow outgoing.

Two "plateau" zones can then be remarked, spaced by an remarkable decrease of the air flow rate when the person is crossing the clear space.

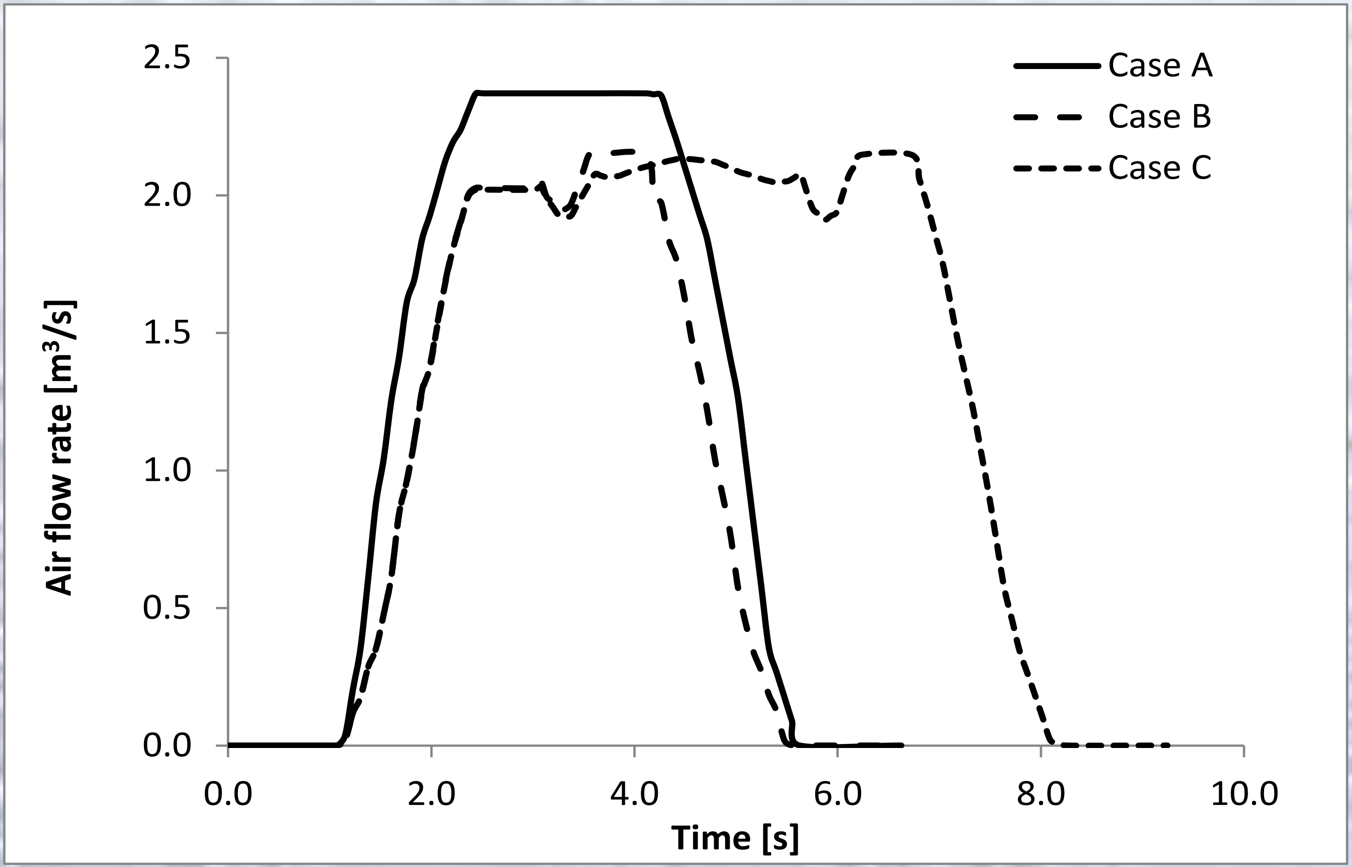

In case C, two "plateau" zones are also detectable from Fig. 7 (dotted line) and spaced by two air flow rate decreasing events, coherently related to the two persons crossing the clear space.

The total air volume outgoing from the room to the corridor was also calculated, during transient conditions for all three cases studied, by a discrete time-integration in post-processing of the air flow rate during time (Fig. 8).

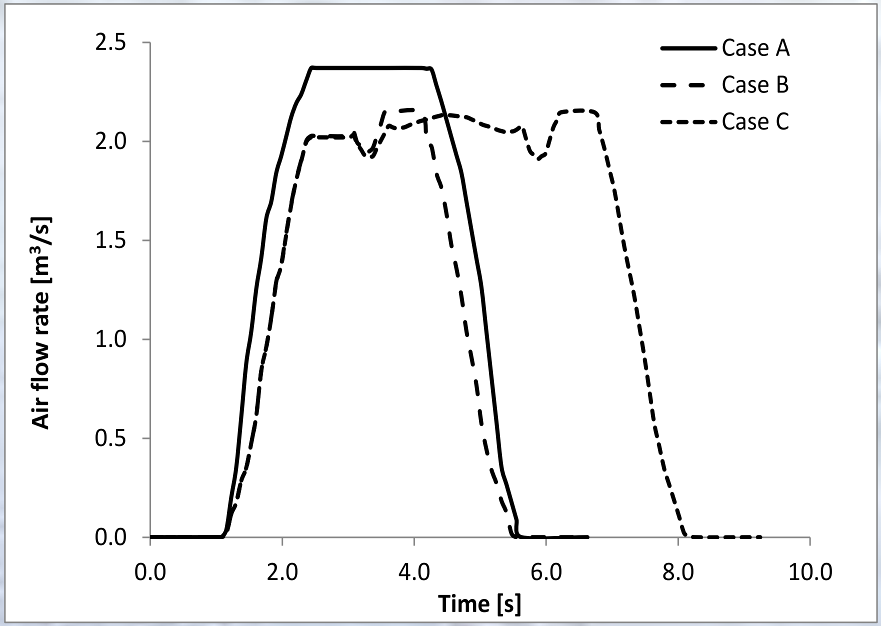

Fig 7 Time evolution of air flow rate throughout the door-space for the three case studies

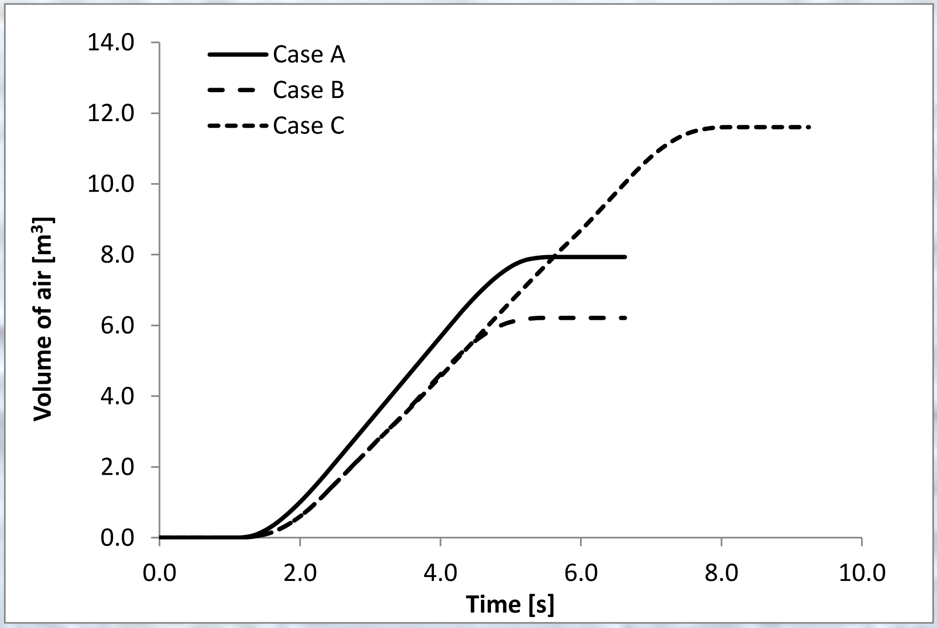

Fig 8 Total volume of air outgoing the OT during the transient analyses for the 3 studied cases

Conclusions

Transient numerical simulations were performed to assess the effect of sliding doors and staff movements on the climate conditions in an ISO5 class OT.

Our study provides a simplified indirect numerical method to simulate the influence of solid objects movement, that exploits analytical expressions to dynamically track the solid-fluid interfaces in the computational domain.

The used turbulence method was preliminary validated by comparing numerical results with experimental data available in literature for similar cases. Other literature evidences were compared to our main findings.

Results highlight a strong modification of the air velocity field inside the OT, due to sliding door and staff movements. Air leakages through the door clear-space were estimated for each configuration.

Conclusions

The introduction of the practice of performing CFD transient simulation on real cases could be an effective, low cost, means of prediction and control.

The provided simulation method can yield significant findings and recommendations for the OT design.

The proposed method contributes to showing that CFD-FEM simulations can provide a basic support for the issues involved in analysis and preventive studies of surgical site infection risk.

THANK YOU FOR YOUR ATTENTION !

Department of Energy Engineering

University of Florence